Protection of IFE First Wall Surfaces from Impulsive Loading by Multiple Liquid Layers

P. Meekunnasombat, J. Oakley, M. Anderson, R. Bonazza

September 2004

UWFDM-1239

Presented at the 16th ANS Topical Meeting on Fusion Energy, 14–16 September 2004, Madison WI.

FUSION TECHNOLOGY INSTITUTE

UNIVERSITY OF WISCONSIN

MADISON WISCONSIN

Protection of IFE First Wall Surfaces from Impulsive Loading by Multiple Liquid Layers

P. Meekunnasombat, J. Oakley, M. Anderson, R. Bonazza

Fusion Technology Institute
University of Wisconsin
1500 Engineering Drive
Madison, WI 53706

http://fti.neep.wisc.edu

September 2004

UWFDM-1239

Presented at the 16th ANS Topical Meeting on Fusion Energy, 14–16 September 2004, Madison WI.

Protection of IFE First Wall Surfaces from Impulsive Loading by Multiple Liquid Layers

P. Meekunnasombat, J. G. Oakley, M. H. Anderson* and R. Bonazza

Fusion Technology Institute, University of Wisconsin – Madison, 1500 Engineering Dr., Madison, Wisconsin, 53706
**manderson@engr.wisc.edu*

A large, vertical shock tube is used to explore the breakup and mitigation effects of liquid layers expected from the hydrodynamic shock generated in an inertial fusion reaction. Single and multiple layers of water are tested at two Mach numbers, 2.12 and 3.20. X-ray radiography techniques are used to image the breakup of the water layer resulting in a quantitative measure of the mass fraction distribution of water after shock impact. The amount of breakup is increased with the addition of multiple layers and the increased breakup decreases the end wall impulse. The speed of the transmitted shock wave can be reduced by 50% and is a weak function of the number of layers. The peak pressure at the end-wall of the shock tube is significantly increased due to the high impulsive force of the single liquid layer, however this pressure is substantially reduced when multiple layers containing the same mass of water are used.

I. INTRODUCTION

Several inertial fusion energy (IFE) reactor designs incorporate liquid jets or sheets[1] (of molten salt[2,3] in many designs) to protect the first wall from neutron and radiation damage and to absorb energy for heat removal from the fuel capsule implosions. Dynamics of flowing liquid sheets have been studied[4,5] and in a reactor chamber these are accelerated by the hydrodynamic shock and the vaporization due to impact and absorption of the energetic particles from the fusion reaction. As a consequence, the impulsive pressure load on the reactor first wall is not exclusively due to the hydrodynamic effects of the shock wave from the fusion reaction, but it is also due to the impact of the shock-accelerated liquid layer. An experimental study of liquid jet columns subjected to a shock wave was performed in a horizontal shock tube along with a numerical study[6]. The numerical results on the side-wall of the shock tube agree well with the experiment, but not at the end-wall since the model did not consider the liquid breakup. However, the end-wall peak pressure from the experiments was found to be 10 times higher due to the momentum of the shock-accelerated liquid. Liquid water has been widely used to experimentally study the dynamics of the molten salt[4,5] because it is much easier to handle and can be scaled[5,7] to molten salt properties. The fragmentation of a liquid jet, resulting from isochoric neutron heating, has been studied theoretically for the HYLIFE reactor design and predictions are made for average fragment diameter[8].

There are two fundamental physics issues that are of interest in liquid wall protection of the first wall. The first is the breakup of the liquid layer which can result in problems with chamber clearing in the case of laser driven systems where the chamber atmosphere allow for laser propagation during repetitive 10Hz shots. The second is the impulsive force associated with the impact of the shock accelerated liquid. Both of these are highly complex issues and in the real case of ICF ignition are dependent on radiation, debris, and hydrodynamics. This paper takes a simple look at just the hydrodynamics of a shock liquid sheet interaction in hopes to understand the basic concept of shock mitigation with the use of liquid layers.

II. EXPERIMENTAL DESCRIPTION

Experiments are conducted in a 9.2 m long vertical shock tube with a square cross-section (25.4 cm sides). The driven section is filled with argon at atmospheric pressure and the water layer is located in the interface section 104 cm above the bottom of the shock tube and 46 cm above the centerline of the test section window. The water layer is supported by a 1 μm thick mylar film, with nylon mono-filament wires for support. Piezoelectric pressure transducers are flush-mounted along the inside wall and the end-wall of the shock tube to measure dynamic pressures inside the tube at a sampling frequency of 2.6 MHz.

An X-ray system is employed as a new diagnostic in the Wisconsin Shock Tube Laboratory for determining the shock-induced breakup of a water layer. A schematic of the X-ray system setup is shown in Fig. 1. Figure 2 is a photograph of the shock tube with the X-ray system setup. A flash X-ray source (Hewlett-Packard Flash X-Ray Electron Beam system, model 43731A) is mounted 15.24 cm from the front window of the test section. The source generates a 70 ns X-ray flash, with a maximum photon energy of 150 KeV, and is aligned with the test section windows (12.7 cm diameter, 0.635 cm thick, T300 grade carbon fiber composite: used in aerospace applications) and projects onto a conversion screen (Kodak Lanex fast screen: used in medical diagnostics) on the other side of the test section. The conversion screen is mounted on a flat board inside a light-proof box. The screen generates a fluorescent flash of green light on the back when it is stimulated by the X-ray photons. The CCD camera inside the box is focused on the screen. The camera shutter is opened approximately 1-2 seconds before the X-ray flash and closed 2-3 seconds after it.

Figure 3 (left) is an X-ray image of an initially 12.8 mm thick water layer 4.5 ms after being accelerated by a *M*=2.12 shock wave. The darker areas indicate where more water is present. This image is converted to water volume fraction as shown in Fig. 3 (right). Detailed explanation for the calibration can be found in Meekunnasombat 2004[9].

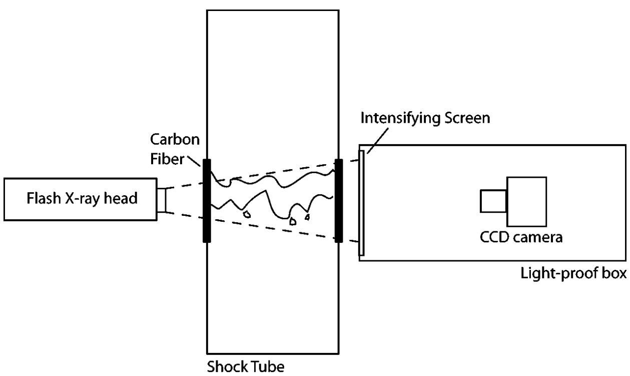

Fig. 1. Schematic of the flash X-ray system with the shock tube and CCD camera

III. RESULTS AND DISCUSSIONS

The end-wall pressure and water volume fraction measurements from the single layer tests are presented in comparison with the multiple layers tests.

III.A. Single Layer

As presented in Meekunnasombat et al. 2003[10], the initially flat, water layer becomes highly unstable when subjected to a shock wave due to shock refraction and the Rayleigh-Taylor hydrodynamic instability. The energy deposited on the water layer during the shock interaction results in the mechanical fragmentation of the layer into a distribution of water droplets. A series of X-ray images of the shocked water layer (initially 12.8 mm thick subjected to a *M*=2.12 shock wave) are recorded and converted to water volume fraction and shown in Fig. 4. The left hand side are the 2-D grayscale maps of water volume fraction of a shocked water layer; and the right hand side are the average volume fractions along vertical position within the region of interest (bordered) shown in the images on the left.

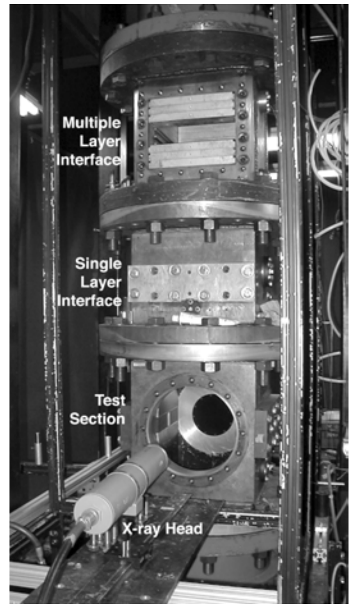

Fig. 2. Photograph of the shock tube with the X-ray system setup.

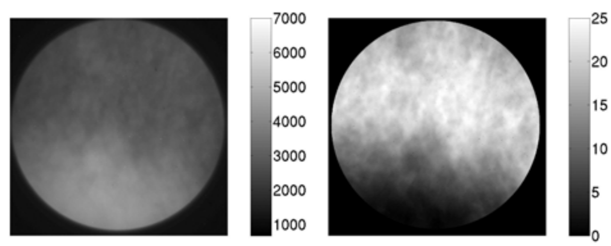

Fig. 3. Left: X-ray image of an initially 12.8 mm thick water layer 4.5 ms after being accelerated by a M=2.12 shock wave. Right: 2-D gray scale map of the volume fraction.

The series are shown in reverse chronological order from the top to visualize the shocked water layer that is moving downward. The leading edge of the shocked water layer is imaged and shown in the bottom image of the figure (Fig. 4A: taken 2.98 ms after the initial shock-layer contact). The body of the water is seen in the second and third figures from the bottom (Fig. 4B and C), taken 3.19 ms and 3.40 ms, respectively, after the contact. The figure at the top (Fig. 4D) shows the trailing edge of the shocked water layer imaged 3.60 ms after the contact. Note that the volume fraction plots for these four separate experiments are visually connected with overlapping areas. These plots are then combined, with the aid of the overlapping areas, yielding a volume fraction plot of the entire span of the shocked water layer as shown in Fig. 5. The result shows that an initially flat water layer is stretched to about 18 times its original thickness (from the beginning of the leading edge to the end of the trailing edge) by a M=2.12 shock wave within 3.2 ms with an average volume fraction of about 12%.

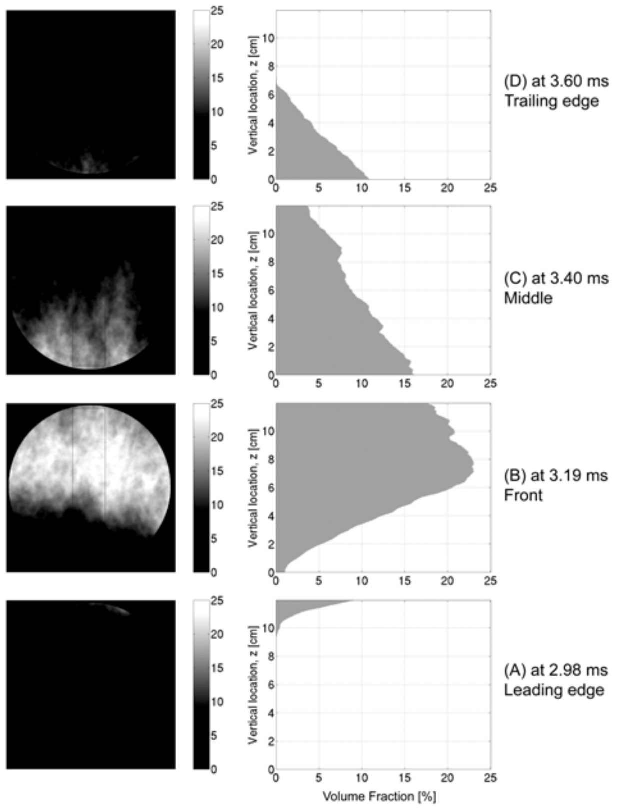

Fig. 4. An initially 12.8 mm thick water layer at M=2.12. Left: 2-D gray scale maps of the volume fraction. Right: Average volume fraction within the region of interest shown in the maps on the left.

Compared with the plot in Fig. 6, where the same water layer (12.8 mm thick) is accelerated by a M=3.20 shock wave from the same initial location (46 cm above the test section), the mixing layer at the higher Mach number is thinner (with an average volume fraction of about 14%) due to its higher velocity, and therefore, a shorter mixing time (1.9 ms versus 3.2 ms).

As discussed in Meekunnasombat *et al*. 2003[10], the presence of the single water layer causes a significantly higher end-wall peak pressure and impulse than those without the water layer. Many IFE chamber designs incorporate multiple liquid layer configuration in order to mitigate the shock more efficiently.

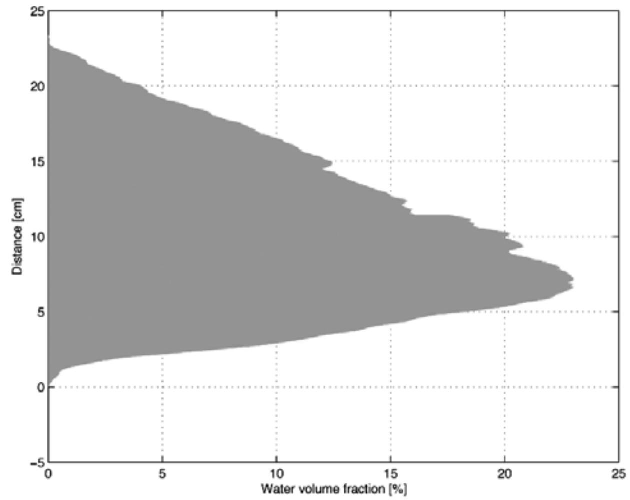

Fig. 5. Percent volume fraction of an initially 12.8 mm thick water layer, approximately 3.2 ms after being accelerated by a M=2.12 shock wave.

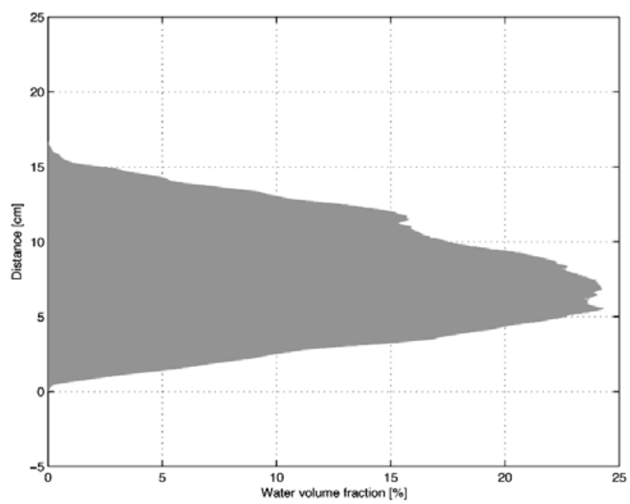

Fig. 6. Percent volume fraction of an initially 12.8 mm thick water layer, approximately 1.90 ms after being accelerated by a M=3.20 shock wave.

Since the X-ray beam cannot be collimated, the parallax effect of the beam causes inaccurate volume fraction measurement when the beam is not perpendicular to the test section and the conversion screen. In other words, the accuracy of the volume fraction measurement reduces as a function of the distance from the center of the test section window. Hence, the areas under the volume fraction plots, such as shown in Fig. 5 and 6, do not exactly equate to the total initial amount of water.

III.B. Multiple Layers

A new interface section containing multiple water layer support frames (up to 9 frames) is installed above the single layer interface section as shown in Fig. 2. The middle of the new multiple layer interface section is 93.5 cm above the middle of the test section and 151.6 cm above the end-wall. Two and three layers of water are tested with different spacings between the layers and the results are compared with the single layer test (at the same distance from the end-wall). To investigate the effects of the multiple water layer's geometry on the end-wall pressure loading, the total volume of water is conserved at 800 cc, i.e., a single 12.8 mm thick layer, two 6.4 mm thick layers, and three 4.2 mm thick layers are tested. The multiple layers tests are conducted at M=2.12 and 3.20 in argon with X-ray radiography imaging.

Figure 7 shows the end-wall pressure histories for a 12.8 mm layer, two 6.4 mm layers and three 4.2 mm layers (with minimum separation between each layer) at M=3.20 (total volume of water of 800 cc kept constant in all cases). The end-wall peak pressure due to the multiple layers is only 30% of that from the single layer.

The end-wall pressure histories are integrated to determine the impulse. The integration times for the impulse calculations are 5 ms and 2.5 ms for M=2.12 and M=3.20, respectively. The end-wall impulses are then compared with the same Mach number without any water layer. Figures 8 and 9 show the change in end-wall impulses, due to the shocked water layer(s), at M=2.12 with spacing S1=1.8 cm (2.0 cm for triple layers) and S2=9.2 cm (9.5 cm for triple layers) between each layer with respect to that without water. The single layer of 12.8 mm thickness yields the highest impulse, (a 30% increase), and the impulses are mitigated to about a 10% increase when the same amount of water is divided into two and three layers. The mitigation becomes less pronounced when the layers are further away from each other, as the results from the spacing S2 show higher impulses than from S1.

The change of the end-wall impulse at M=3.20 is shown in Fig. 8. The trend is similar to that for M=2.12, except that now the impulse is mitigated to about 20% *lower* than that for the test without the water layer, with the multiple layer configurations. Hence, from these end-wall pressure data, it can be concluded that separating the water layer into multiple layers can significantly reduce the end-wall pressure loading.

Figures 10A and 10B show the comparison of the water volume fraction between the single and double layer configurations at about 5 ms after being accelerated by a M=2.12 shock wave. The measured volume fraction of the shocked multiple water layers seems to be rather random compared to that of the single layer. As shown in Fig. 10B from the two-layer configuration (6.4 mm thick each) with small spacing between the layer (S1=18.3 mm) at M=2.12, the overall volume fraction is significantly lower than that from the single layer (Fig. 10A) with an asymmetric breakup structure. A similar asymmetric structure of the mixing layer is also found with a larger spacing between the layers (S2= 92.4 mm) with slightly higher volume fraction than for the small spacing case.

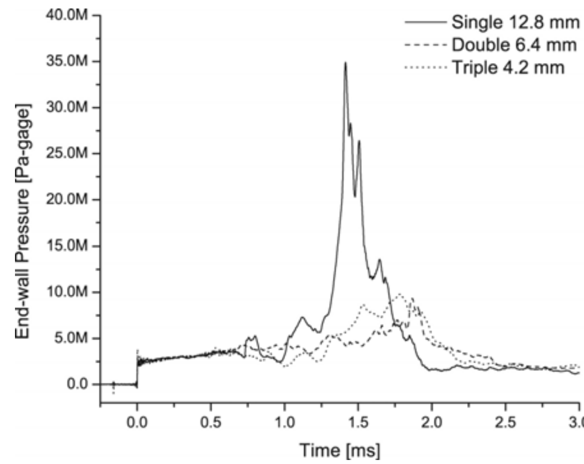

Fig. 7. End-wall pressure history comparison for a 12.8 mm layer, two 6.4 mm layers and three 4.2 mm layers at M=3.20.

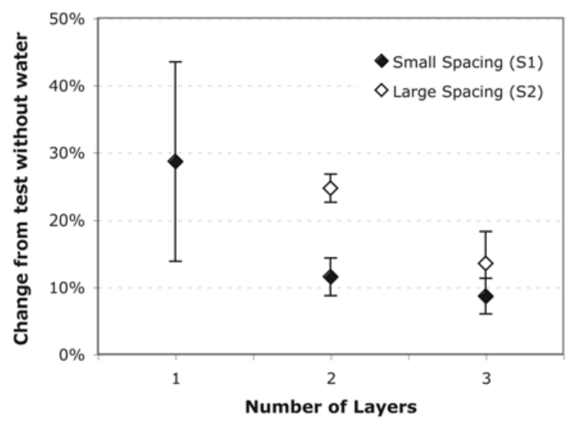

Fig. 8. Percent increase of the end-wall impulse from the test without water at M=2.12. The total volume of the water layers is conserved at 800 cc.

Although the multiple layer configurations mitigate the end-wall pressure load due to the accelerated liquid layer, the volume fraction measurements show that the water layers break up more (wider span and lower average volume fraction) in the multiple layer configurations. This indicates that more energy is dissipated in the breakup process and results in lower end-wall pressure loads with the assist of multiple-layer configurations. The reduced lower pressure load is a favorable result for the reactor life, but the greater breakup of the liquid protection could be a potential issue in the design of the chamber clearing system for laser driven systems.

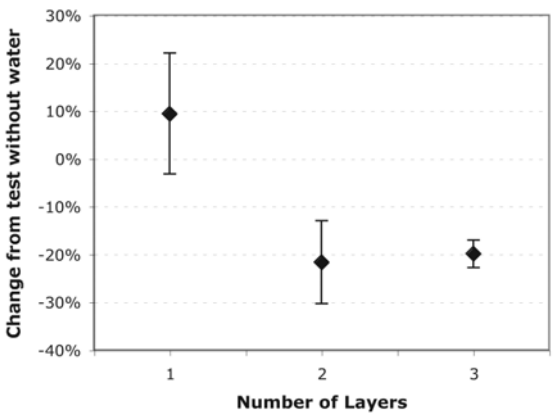

Fig. 9. Change of the end-wall impulse departs from the test without water at M=3.20. The total volume of water layer is conserved at 800 cc.

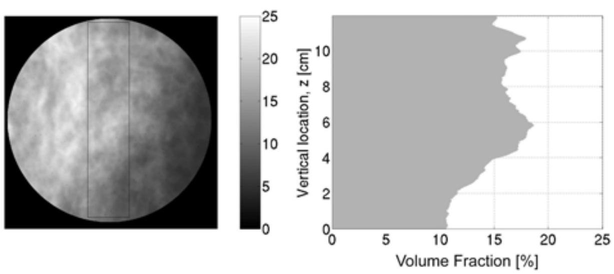

(A)

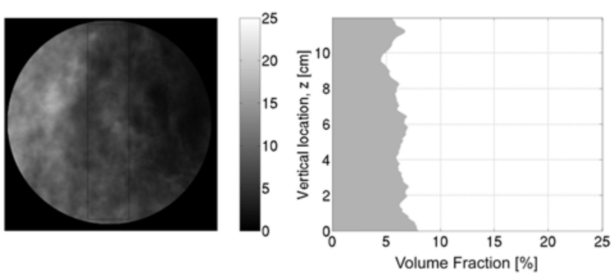

(B)

Fig. 10. Water volume fraction after being accelerated by a M=2.12 shock wave of (A) an initially 12.8 mm thick layer at 4.93 ms and (B) two layers initially 6.4 mm thick (18.3 cm apart) at 5.18 ms.

IV. CONCLUSIONS

Flash X-ray radiography enables quantitative measurement of the shocked water layer volume fraction. It is found that the shock-induced spread of the liquid layer develops very rapidly—to 18 times its original thickness within 3.2 ms at M=2.12 with maximum volume fraction of 23%. The spread near the leading edge of the shocked layer is smaller than that near the trailing edge.

More than a 50% decrease in end-wall peak pressure is observed when the same amount of water is divided into two layers with a small spacing in between. The results from two and three layers are not significantly different. At M=3.20, the end-wall impulse decreases to less than that in the test without water, when the water is divided into two and three layers. The strength of the transmitted shock wave is nearly unchanged when the water is divided into multiple layers. The multiple-layer configurations reduce the end-wall pressure load, which is favorable in the IFE reactor, but also increase the breakup and droplet formation, which could be an issue in the design of the chamber clearing system.

ACKNOWLEDGMENTS

[1] R. W. MOIR et al., “H Funding for this work was provided by the U. S. Department of Energy under contract number DE-FG02-97ER54413.

REFERENCES

[1] R. W. MOIR et al., “HYLIFE-II: A molten-salt inertial fusion energy power plant design-Final report,” *Fusion Tech*, Vol. 25 p. 5 (1994).

[2] H. MORIYAMA, “Chemical behaviors of tritium formed in a LiF-BeF2 mixture,” *J. of Nuclear Materials*, Vol. 148 p. 211 (1986).

[3] T. TERAI et al., “Tritium release from Li2BeF4 molten salt breeder under neutron irradiation at elevated temperature,” *Fusion Tech*, Vol. 39 n. 2-2 p. 768 (2001).

[4] P. F. PERTERSON, “Design methods for thick-liquid protection of inertial fusion chambers,” *Fusion Tech*, Vol. 39 n. 2-2 p. 702 (2001).

[5] S. J. PEMBERTON, *Thick Liquid Protection in Inertial Fusion Power Plants,* Ph.D. thesis, University of California-Berkeley (2002).

[6] J. C. LIU, *Experimental and Numerical Investigation of Shock Wave Propagation Through Complex Geometry, Gas Continuous, Two-phase Media*, Ph.D., UC-Berkeley (1993).

[7] C. JANTZEN and P. F. PETERSON, “Scaled Impulse Loading for Liquid Hydraulic Response in IFE Thick-liquid chamber experiments,” *Nuclear Inst & Methods in Phys Research*, Vol. A 464 p. 404 (2001).

[8] J. BLINK and W. HOOVER, “Fragmentation of Suddenly Heated Liquids in ICF Reactors,” *Fusion Tech*, Vol. 8 pp. 1844-1849 (1985).

[9] P. MEEKUNNASOMBAT *et al,* “Experimental Investigation of a Shock-accelerated Liquid Layer with Imaging and Pressure Measurement,” *Fusion Sci & Tech*, Vol. 44 pp. 351-355 (2003).

[10] P. MEEKUNNASOMBAT, Ph.D. thesis, University of Wisconsin-Madison (2004).